Default mode and primary visual network coupling is associated with increased mind-wandering frequency in Parkinson's disease with visual hallucinations

Ishan C. Walpola,[1] Alana J. Muller,[1] Julie M. Hall,[1,2] Jessica R. Andrews-Hanna,[3] Muireann Irish,[1,4,5] Simon J. G. Lewis,[1] James M. Shine[1] and Claire O'Callaghan[1,6]

[1] Brain and Mind Centre, University of Sydney, Sydney, Australia
[2] School of Social Sciences and Psychology, Western Sydney University, Sydney, Australia
[3] Institute of Cognitive Science, University of Colorado Boulder, Boulder, CO
[4] Australian Research Council Centre of Excellence in Cognition and its Disorders, Sydney, Australia
[5] School of Psychology, University of Sydney, Sydney, Australia
[6] Department of Psychiatry and Behavioural and Clinical Neuroscience Institute, University of Cambridge, Cambridge, UK

Corresponding author
Claire O'Callaghan
Herchel Smith Building for Brain & Mind Sciences, Cambridge Biomedical Campus, Cambridge CB2 0SZ, UK
(+44) 1223-764420; co365@cam.ac.uk

Short title: Mind-wandering in PD visual hallucinations

Keywords: Parkinson's disease; Visual hallucinations; Mind-wandering; Default mode network; Primary visual cortex; Resting state functional magnetic resonance imaging

Word count abstract: 250 Word count main text:
Figures: 6 Tables: 2
Supplementary figures: 4

Abstract

Background: An imbalance between top-down expectations and incoming sensory information is implicated in the genesis of hallucinations across neuropsychiatric disorders. In Parkinson's disease (PD) with visual hallucinations, over-activity in the default mode network (DMN) is a hypothesised source of excessive top-down influence that can dominate visual perception.

Methods: In 38 PD patients (18 with hallucinations; 20 without) and 20 age-matched controls, we administered a validated thought-sampling task to establish whether PD hallucinators experienced increased mind-wandering – a form of spontaneous thought strongly associated with DMN activity. Neural correlates of the behavioural differences in mind-wandering frequency were established via resting-state functional connectivity and voxel-based morphometry analyses.

Results: PD hallucinators (PD+VH) exhibited significantly higher mind-wandering frequencies compared to non-hallucinators (PD-VH), who showed reduced levels relative to controls. Inter-network connectivity and seed-to-voxel analyses confirmed increased mind-wandering in PD+VH was associated with greater coupling between the DMN and primary visual cortex (V1). In contrast, reduced mind-wandering was associated with grey matter loss in the left posterior parietal cortex in PD-VH.

Conclusions: Elevated mind-wandering associated with DMN-visual network coupling emerged as a distinguishing feature of PD hallucinators. We propose that increased mind-wandering reflects excessive spontaneous thought and mental imagery, which can furnish the content of visual hallucinations. DMN-V1 coupling may provide a neural substrate by which regions of the DMN exert disproportionate influence over ongoing visual perception. Our findings refine current models of visual hallucinations by identifying a specific cognitive feature and neural substrate consistent with the excessive top-down influences over perception that lead to hallucinations.

Introduction

Hallucinations that are predominantly visual in nature affect over 40% of patients in the early stages of Parkinson's disease (PD), and upwards of 80% as the disease progresses (ffytche *et al.*, 2017). PD visual hallucinations have been associated with increased activity and connectivity in the default mode network (DMN), both in the resting state (Yao *et al.*, 2014, Franciotti *et al.*, 2015) and during visual misperceptions (Shine *et al.*, 2015b). One interpretation of these findings is that an over-active DMN may dominate the perceptual processes in a top-down manner, supplying internally generated imagery that overrides the flow of incoming sensory information (Powers *et al.*, 2016, O'Callaghan *et al.*, 2017b).

Models of PD visual hallucinations posit that in the context of poor quality visual input – due to the attentional impairments, visual deficits and retinal pathology that can occur in PD (Weil *et al.*, 2016) – higher-order regions involved in the generation of mental imagery and perceptual expectancies exert excessive influence upon perception (Collerton *et al.*, 2005, Diederich *et al.*, 2005, Shine *et al.*, 2014). The imbalance between top-down influences and incoming sensory input can be interpreted in a Bayesian predictive coding framework, in which increasing precision (i.e., weighting) is afforded to prior beliefs (i.e., top-down expectations or predictions), such that they override incoming sensory evidence and dominate the ultimate percept (Friston, 2005, Fletcher and Frith, 2009, Adams *et al.*, 2013). Indeed, in PD with visual hallucinations, accumulation of sensory evidence is slow and inefficient, and is therefore less informative, which may cause it to be down-weighted in favour of perceptual priors (O'Callaghan *et al.*, 2017a).

The hierarchical nature of the brain's visual processing system supports the reciprocal feed-forward and feed-back flow of information between early visual regions and higher-order regions across the cerebral cortex (Gilbert and Li, 2013). More specifically, regions within the DMN have been identified as sources of top-down influence over visual perception. These regions include the medial prefrontal cortices, which use early low spatial frequency information to generate expectations that constrain ongoing visual processing (Bar *et al.*, 2006, Summerfield *et al.*, 2006, Kveraga *et al.*, 2007); hippocampal pattern completion mechanisms supply memory-

based expectations to the visual cortex (Hindy *et al.*, 2016); parahippocampal and retrosplenial cortices support the rapid activation of contextual associations during visual processing (Kveraga *et al.*, 2011, Aminoff *et al.*, 2013); and, distinct populations of neurons in the inferior temporal cortex encode predictions and prediction errors in relation to incoming visual input (Bell *et al.*, 2016, Kok, 2016). Yet despite a number of established routes by which the DMN may influence visual perception, and evidence of unconstrained DMN activity in PD with visual hallucinations, we know very little about the behavioural consequences of an over-engaged DMN and how this might contribute to hallucinations.

In keeping with its role as a source of top-down influence over visual perception, the DMN has been implicated in many cognitive processes relevant for generating expectations about the sensory environment, including mental imagery and scene construction, autobiographical memory, prospection, and retrieval of contextual associations (Buckner *et al.*, 2008, Spreng *et al.*, 2009, Andrews-Hanna *et al.*, 2010, Kveraga *et al.*, 2011, Schacter *et al.*, 2012). One common experience that draws upon the aforementioned cognitive processes, and is strongly linked to activity in the DMN, is mind-wandering. Mind-wandering can be characterised by thoughts that are decoupled from the immediate perceptual environment and unrelated to ongoing task demands (Smallwood and Schooler, 2015, Seli *et al.*, 2018). Current frameworks further emphasise that mind-wandering is a mental state that arises spontaneously, in which thoughts are unguided and unconstrained (Christoff *et al.*, 2016, Irving, 2016).

There is a striking similarity between certain core characteristics of both mind-wandering and visual hallucinations: they are both transient forms of spontaneous cognition that are relatively unconstrained by sensory input, and are underpinned by dynamic shifts in the interactions within and between similar large-scale brain networks (Christoff *et al.*, 2016, Collerton *et al.*, 2016, Zabelina and Andrews-Hanna, 2016, Kucyi, 2017). Given this shared phenomenology and evidence for an overlapping neural basis, we predicted that clinical subgroups with visual hallucinations would also show changes in their propensity for mind-wandering. Whilst such definitive studies have not been conducted to date, in patients with schizophrenia higher frequencies of mind-wandering have been observed, correlating with the severity of their positive symptoms, including hallucinations (Shin *et al.*,

2015). Previous work in PD has demonstrated that individuals with visual hallucinations exhibit stronger mental imagery – a prominent feature of mind-wandering – during a binocular rivalry paradigm (Shine *et al.*, 2015a). Together these findings suggest that increased mind-wandering may represent a neurocognitive marker for various hallucinatory phenomena across diseases.

To address the question of whether mind-wandering is related to hallucinations in PD, the present study utilised a validated thought sampling task designed for use in clinical populations with cognitive impairment (O'Callaghan *et al.*, 2015). Using this task, we measured mind-wandering frequencies in PD patients with (PD+VH) and without (PD-VH) visual hallucinations, and healthy controls. To explore the neural correlates of mind-wandering frequency, we employed network-level and seed-to-voxel analysis of resting-state functional MRI (rsfMRI) in the PD cohort. Of specific interest were the between-group differences in the association between mind-wandering frequency and network interactions. We predicted that connectivity between the DMN and visual areas would be related to elevated mind-wandering in patients with visual hallucinations. Using voxel-based morphometry, we further examined grey matter correlates of mind-wandering frequency, to determine whether the large-scale network functional connectivity patterns associated with both mind-wandering and PD hallucinations, would also be reflected in patterns of grey matter loss. Taken together, we aimed to establish whether elevated mind-wandering and its associated neural correlates may be identifiable traits in a population prone to visual hallucinations.

Methods and Materials

Case selection

Thirty-eight individuals with PD were recruited from the Parkinson's disease research clinic, University of Sydney, Australia. Individuals were identified as hallucinators if they self-reported visual hallucinatory phenomena and scored ≥1 on question two (the hallucinations item) of the MDS-UPDRS (Goetz *et al.*, 2008). This resulted in 18 PD patients with hallucinations and 20 without hallucinations.

All individuals with PD satisfied the United Kingdom Parkinson's Disease Society Brain Bank criteria for PD and were not demented, scoring above the recommended cut-off of ≥ 26 on Montreal Cognitive Assessment (MoCA) (Dalrymple-Alford *et al.*, 2010). To determine motor severity, patients were assessed on the Hoehn and Yahr Scale and the motor section of the unified Parkinson's disease rating scale (UPDRS-III). Mood was assessed via the self-reported Beck Depression Inventory-II (BDI-II) (Beck *et al.*, 1996). General neuropsychological measures were administered to assess working memory (backwards digit-span), attentional set-shifting (Trail Making Test, Part B minus Part A), and memory (story retention on the Logical Memory component of the Wechsler Memory Scale). All clinical and neuropsychological assessments, as well as neuroimaging, were performed with participants on their regular antiparkinsonian medication. Dopaminergic dose equivalence (DDE) scores were calculated, and no one in the cohort was taking antipsychotic medication or cholinesterase inhibitors. All individuals with PD underwent neuroimaging to acquire T1-weighted structural images and resting-state blood-oxygenation level dependent (BOLD) functional scans.

Twenty age- and education-matched healthy controls, screened for a history of neurological or psychiatric disorders, were assessed on the mind-wandering task. The study was approved by the local Ethics Committees and all participants provided informed consent in accordance with the Declaration of Helsinki. See Table 1 for demographic details and clinical characteristics.

Mind-wandering experimental task & scoring procedures

The task involved 9 trials. In each trial, a 2-dimensional coloured shape (e.g., blue square, yellow circle, etc.) was presented on the screen for varying durations (Short: ≤20 s, Medium: 30-60 s, Long: ≥90 s). After each shape was presented, the participant was prompted to describe aloud what they were thinking about during the presentation of the shape stimulus.

Participants' reported thoughts were scored on a continuum, ranging from Level 1 to Level 4. Level 1 represents tightly stimulus-bound thought, including thinking about the stimulus, i.e., "a blue square," or thinking of "nothing". In contrast, Level 4 responses represent stimulus-independent thought, or mind-wandering. These

thoughts bear no obvious relationship to the stimulus or the task at hand, or the immediate testing environment. Level 2 and 3 represent intermediary responses, which do not qualify as fully-fledged instances of mind-wandering as they still bear a relationship to the presented stimulus or immediate environment. See Figure 1 and see Supplementary Material for a detailed description of the scoring levels and example responses.

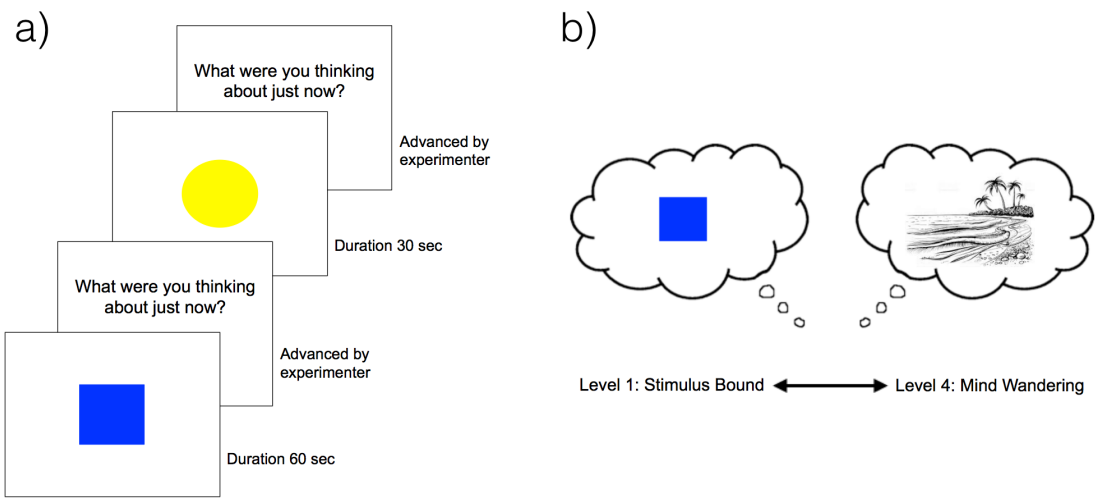

Figure 1. ***Task structure and schematic of scoring system.*** a) An example of two trials in the thought sampling task; b) Responses were scored from 1-4, with 1 consisting of a stimulus bound response, such as reporting thoughts about the displayed shape, and 4 corresponding to thoughts completely unrelated to the task or immediate environment.

The final score awarded for each trial was the highest level achieved on that trial, ranging from 1-4. Instances of each scoring level achieved were counted across the 9 trials, and transformed into a total percentage for each level achieved over the course of the task (i.e., total instances of levels 1, 2, 3 or 4 divided by 9 multiplied by 100). The primary analysis was focused on differences in mind-wandering frequency between PD with hallucinations (PD+VH), PD without hallucinations (PD-VH), and controls. Therefore, the proportion of Level 4 responses – referred to as the mind-wandering frequency – was compared across the groups and further analysed as a covariate in the neuroimaging analyses. Secondary behavioural analyses were conducted to determine overall performance of the three groups on the task. This

involved comparing the proportion of responses that each group achieved on all four scoring levels of the task.

Statistical analysis

Analyses were performed in R version 3.3.1 (http://www.r-project.org/). Two-sided Welch's Independent samples *t*-tests and one-way ANOVAs with Tukey *post hoc* tests compared demographics and background clinical measures. For performance on the mind-wandering task, homogeneity of variance was verified using Levene's test and values were checked for normality by inspection of normal Q-Q plots and the Shapiro-Wilk test. To reduce skew in the data, a square root transformation was applied to the mind-wandering scores. Performance on the mind-wandering task was then analysed using mixed-effects ANOVAs, implemented in the "lme4" package (Bates *et al.*, 2014). Where appropriate, group, score level and trial duration were specified as fixed effects, and subject was entered as a random effect. Where a factor only had three levels, post hoc analysis of significant main effects was performed using the Fisher's Least Significant Difference (LSD) procedure (Cardinal and Aitken, 2013). Where factors had more than three levels, main effects were analysed using post-hoc t-tests with the Sidak correction for multiple comparisons. In these cases, post-hoc analyses of interactions were conducted using separate univariate ANOVAs to establish simple effects. Plots were created using the "yarrr" package (Phillips, 2016). Scripts for the behavioural analysis are available at https://github.com/claireocallaghan/MindWandering_PD_VH.

Imaging acquisition

The 38 individuals with PD underwent magnetic resonance imaging (MRI). Imaging was conducted on a 3T MRI (General Electric, Milwaukee, USA). Whole-brain three dimensional T1-weighted sequences were acquired as follows: coronal orientation, matrix 256 x 256, 200 slices, 1 x 1 mm^2 in-plane resolution, slice thickness 1 mm, TE/TR = 2.6/5.8 ms. T2*-weighted echo planar functional images were acquired in interleaved order with repetition time (TR) = 3 s, echo time (TE) = 32 ms, flip angle 900, 32 axial slices covering the whole brain, field of view (FOV) = 220 mm, interslice gap = 0.4 mm, and raw voxel size = 3.9 x 3.9 x 4 mm thick. Each resting state scan lasted 7 min (140 TRs). During the resting-state scan, patients were instructed to lie awake with their eyes closed.

Resting state fMRI preprocessing and motion correction

Functional magnetic resonance imaging (fMRI) preprocessing and analysis was performed using Statistical Parametric Mapping software (SPM12, Wellcome Trust Centre for Neuroimaging, London, UK, http://www.fil.ion.ucl.ac.uk/spm/software/). We used a standard preprocessing pipeline that included slice-timing correction, rigid body realignment, spatial smoothing with a Gaussian kernel (FWHM) of 6mm, and all anatomical scans were registered to the Montreal Neurological Institute standard brain space. Preprocessed images were imported into CONN: The Functional Connectivity toolbox (https://www.nitrc.org/projects/conn) in MATLAB for all functional connectivity analyses.

To compensate for motion-related artifacts (Power *et al.*, 2012), we performed a quality control measure known as scrubbing to effectively remove time points with excessive head motion (i.e., framewise displacement in x, y, or z direction > 2 mm from the previous frame; global intensity > 9 standard deviations from mean image intensity of the entire resting state scan). This approach (Artifact Detection Tools; https://www.nitrc.org/projects/artefact–detect/) effectively removes outlier scans by including them as dummy-coded regressors during the de-noising procedure, so as to avoid discontinuities in the time-series. We also tested for significant differences in maximum motion or scans scrubbed between the PD+VH and PD-VH groups. No significant differences were found in maximum framewise displacement (p = 0.50), maximum scans scrubbed (p = 0.25), mean framewise displacement (p = 0.59), or mean scans scrubbed (p = 0.25). Other noise sources in the BOLD signal (i.e., from white matter and cerebrospinal fluid) were corrected for by using a principle component-based 'CompCor' method (Whitfield-Gabrieli and Nieto-Castanon, 2012). We applied a band-pass filter (0.008 - 0.09 Hz) to limit the effect of low-frequency drift and high-frequency noise on the BOLD signal time-series.

Relationship between inter-network functional connectivity and mind-wandering frequency

To assess differences in the association between mind-wandering frequency and inter-network functional connectivity between the two PD groups, we used 12 individual intrinsic connectivity network "regions of interest", which were defined on a

functional basis (Shirer *et al.*, 2012). The networks included in our analysis are shown in Figure 4a. We did not include the auditory or language networks, as the auditory network is not implicated in network-based models of visual hallucinations and, as others have noted, there is substantial overlap between the language network and aspects of the default mode/limbic networks (Zabelina and Andrews-Hanna, 2016). We corrected for multiple comparisons by using a False Discovery Rate (FDR) threshold of $p < 0.05$.

Based on the results from the analysis described above, we performed a post-hoc seed-to-voxel functional connectivity analysis. This was to investigate whether between-group differences (i.e., PD+VH vs. PD-VH) in the association between mind-wandering and primary visual network (V1) functional connectivity extended beyond the dorsal default mode network. We calculated a correlation between the average filtered BOLD signal in V1 and all other voxels in the brain for both groups (PD+VH and PD-VH). Then, a between-group contrast of the regression coefficient, capturing the association between mind-wandering frequency and seed-to voxel functional connectivity, was carried out with a height threshold of $p < 0.001$ and a cluster-size threshold of $p < 0.05$, corrected using FDR. Seed-to-voxel statistical tests for this post-hoc analysis were one-sided, as we were specifically interested in the spatial boundaries of increased V1 connectivity.

Voxel-based morphometry preprocessing

Voxel-based morphometry (VBM) was performed using the FMRIB software library package FSL (http://www.fmrib.ox.ac.uk/fsl/). Scans were skull-stripped using the BET algorithm (Smith, 2002) and tissue segmentation was completed using FMRIB's Automatic Segmentation Tool (FAST v4.0) (Zhang *et al.*, 2001). A study-specific grey matter template was created using the maximum equal number of scans from both groups (18 from each) and registered to the Montreal Neurological Institute Standard space (MNI 152) using a non-linear b-spline representation of the registration warp field. Grey matter partial volume maps were non-linearly registered to the study template and modulated by dividing by the Jacobian of the warp field, to correct for any contraction/enlargement caused by the non-linear component of the transformation. After normalisation and modulation, the grey matter maps were smoothed with an isotropic Gaussian kernel with a sigma of 2 mm.

Relationship between grey matter volume and mind-wandering frequency

To examine the relationship between grey matter volume and mind-wandering frequency, a GLM was conducted combining the PD+VH and PD-VH groups, and entering the mind-wandering frequency score as a covariate in the design matrix, using FSL's randomise. Interaction and main effects were examined using four contrasts: 1) [0 0 -1 1] and 2) [0 0 1 -1] to test for interactions; 3) [0 0 1 1] and 4) [0 0 -1 -1] to test for main effects. Results were corrected for cluster mass, at $p < 0.05$ and a cluster forming threshold of T = 3.

Goodness of fit

To determine spatial similarity between clusters where there was a significant relationship between grey matter intensity and mind-wandering frequency, and the intrinsic functional networks from the Stanford atlas, goodness of fit scores (GOF) were derived using the following formula (Guo *et al.*, 2016).

$$\text{GOF} = (V_{in} - V_{out}) \,/\, (V_{in} + V_{out}) \qquad (1)$$

Where V_{in} = probability of voxels in the group-difference map to be inside of the connectivity network; and V_{out} = probability of voxels in the group-difference map to be outside of the connectivity network. Values were re-scaled to give GOF probabilities between 0-1.

Results

Demographics, clinical characteristics and background neuropsychology

PD and control groups were matched for age and education [age: F(2,55) = 2.07, p = 0.17; education: F(2,55) = 1.37, p = 0.26]. PD+VH and PD-VH groups were matched on clinical variables, including global cognition [MoCA: t(34.49) = -0.24, p = 0.81], years of disease duration [t(28.51) = -1.41, p = 0.17], daily dopamine medication levels [DDE: t(36) = -1.041, p = 0.30], disease stage and motor severity [Hoehn and Yahr: t(27.98) = -0.44, p = 0.66; UPDRS III: t(33.34) = -1.06, p = 0.30], and depression levels [t(26.81) = -1.28, p = 0.21]. However, PD+VH performed worse than PD-VH on measures of attentional set-shifting and memory retention [TMT B-A:

t(21.75) = -2.87, p < 0.01; Logical memory % retention: t(27.67) = 2.395, p < 0.05]. Working memory performance did not differ between the patient groups [Digit span backward: t(32.44) = -0.73, p = 0.47]. See Table 1.

Table 1. Mean (standard deviation) values for demographics, clinical characteristics and background neuropsychology.

Demographics, clinical characteristics & general neuropsychology	**Controls**	**PD+VH**	**PD-VH**	***p* value**
N	20	18	20	-
Sex (M:F)	12:8	14:4	17:3	-
Age	67.3 (6.4)	67.5 (6.7)	63.7 (6.6)	n.s.
Education	14.7 (2.6)	13.3 (3.3)	14.6 (2.4)	n.s.
MoCA	-	27.9 (1.3)	27.9 (1.1)	n.s.
Duration (yrs diagnosed)	-	7.6 (5.0)	5.7 (3.2)	n.s.
DDE (mg/day)	-	832.8 (395.7)	691.5 (440.5)	n.s.
Hoehn & Yahr stage	-	2.2 (.57)	2.1 (.36)	n.s.
UPDRS III	-	33.4 (15.9)	28.4 (13.4)	n.s.
BDI-II	-	11.6 (10.2)	8.1 (5.9)	n.s.
Neuropsychology				
TMT B-A (seconds)	-	76.6 (57.3)	35.2 (22.7)	**
Digit span backward	-	7.0 (1.6)	6.6 (2.3)	n.s.
Logical memory % retention		75.6 (17.7)	87.1 (10.9)	*

n.s. = non significant; ** = p < .01; * = p < .05.
MoCA = Montreal Cognitive Assessment; DDE = Dopaminergic dose equivalence; BDI-II = Beck Depression Inventory-II; TMT B-A = Trail Making Test part B minus part A.

Hallucinators have a higher frequency of mind-wandering compared to non-hallucinators

As shown in Figure 2, mind wandering occurred significantly more frequently in hallucinators than non-hallucinators. There was a main effect of group [F(2,55) = 4.38, $p < 0.05$], and post-hoc comparisons revealed that controls and PD+VH did not differ, but they both showed higher frequencies of mind-wandering than the PD-VH group (Fisher's LSD, $p < 0.05$).

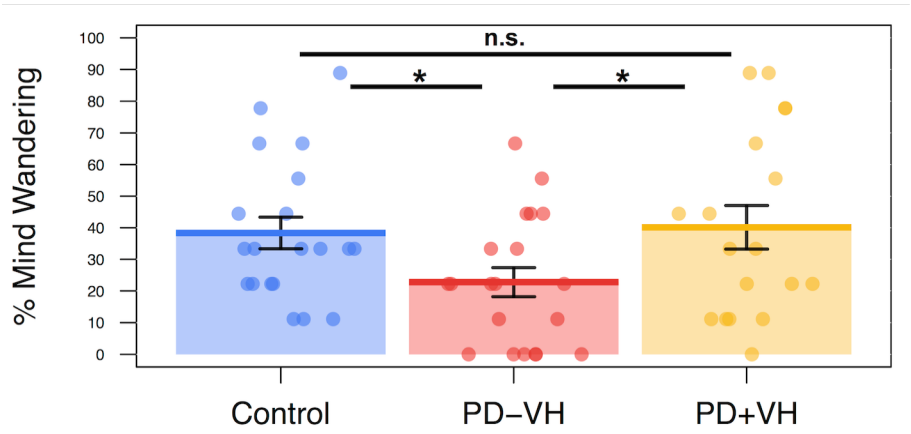

Figure 2. ***Mind-wandering frequency.*** PD with hallucinations (PD+VH) and controls both showed higher frequencies of mind-wandering (i.e., had significantly more Level 4 responses on the thought sampling task) compared to non-hallucinators (PD-VH). Error bars show standard error of the mean; n.s. = not significant; * = $p < .05$.

Overall performance on the mind-wandering task revealed that significant group differences emerged exclusively for mind-wandering responses

Figure 3 shows the frequency of responses across all scoring levels, ranging from Level 1 (stimulus-bound thought) to Level 4 (mind-wandering). No significant main effect of group was evident [$F(2,220) = 0.45$, $p = 0.64$], however, a significant main effect of response level [$F(3,220) = 14.47$, $p < 0.001$] was observed. Post hoc t-tests with Sidak correction showed that, regardless of group, higher frequencies of Levels 2, 3 and 4 responses were obtained, relative to Level 1 (p values < 0.01). The other Levels did not differ significantly from each other (p values > 0.05).

The Level x Group interaction was marginally significant [$F(6,220) = 2.13$, $p = 0.05$]. We followed this interaction with tests of simple effects, to determine whether the groups differed in their response frequencies at any Level apart from Level 4, which we showed in our focused analysis above. Follow-up tests of simple effects revealed the frequency of responses across the groups did not differ significantly for Level 1 [$F(2,55) = 1.28$, $p = 0.29$], Level 2 [$F(2,55) = 1.14$, $p = 0.33$] or Level 3 [$F(2,55) = 0.19$, $p = 0.83$]. The groups only differed significantly in their Level 4 responses (i.e., % mind-wandering frequency) [$F(2,55) = 4.38$, $p < 0.05$]. In addition, all groups showed an increased tendency towards mind-wandering on longer trials (See

Supplementary material and Figure S1 for analyses and results), replicating previous studies using the task (Geffen *et al.*, 2017, O'Callaghan *et al.*, 2017).

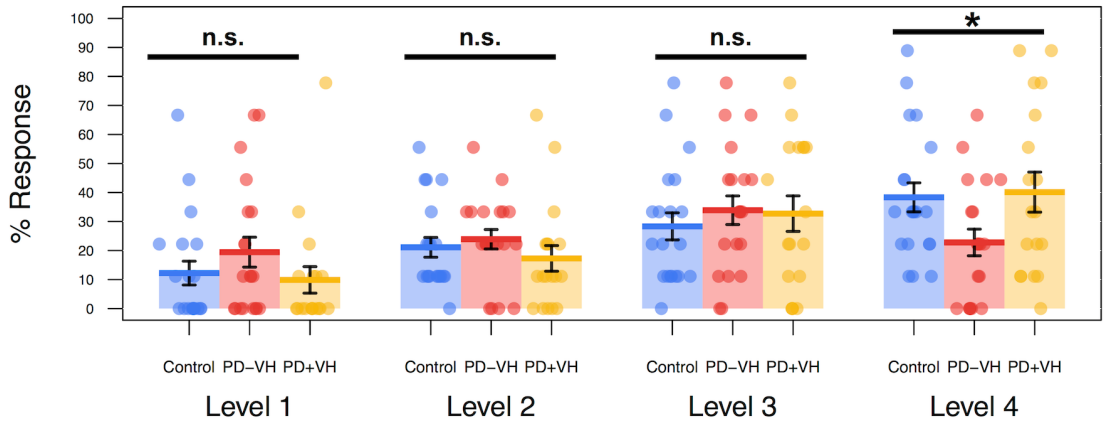

Figure 3. ***Frequency of responses at each of the four scoring levels***. Group differences were only found for Level 4 responses (i.e., mind-wandering frequency). Frequencies of responses across the three groups were not significantly different for Levels 1, 2 and 3. Error bars show standard error of the mean; PD-VH = non-hallucinators; PD+VH = hallucinators; n.s. = not significant; * = $p < 0.05$.

A stronger association between V1-dDMN inter-network coupling and mind-wandering frequency in PD+VH vs. PD-VH

Results of the inter-network coupling analysis were consistent with our predicted default mode-visual network association with mind-wandering in hallucinating individuals. Of all network pairs (Figure 4a), only the association between increased primary visual network and the dorsal default mode network functional connectivity (i.e., V1-dDMN coupling) and mind-wandering frequency differed significantly between groups ($p < 0.05$, FDR; Figure 4b). PD+VH had a significantly stronger association between mind-wandering frequency and V1-dDMN coupling as compared with PD-VH. Post-hoc Tukey box-and-whisker plots did not detect any outliers in the V1-dDMN coupling results (See Supplementary material and Figure S2).

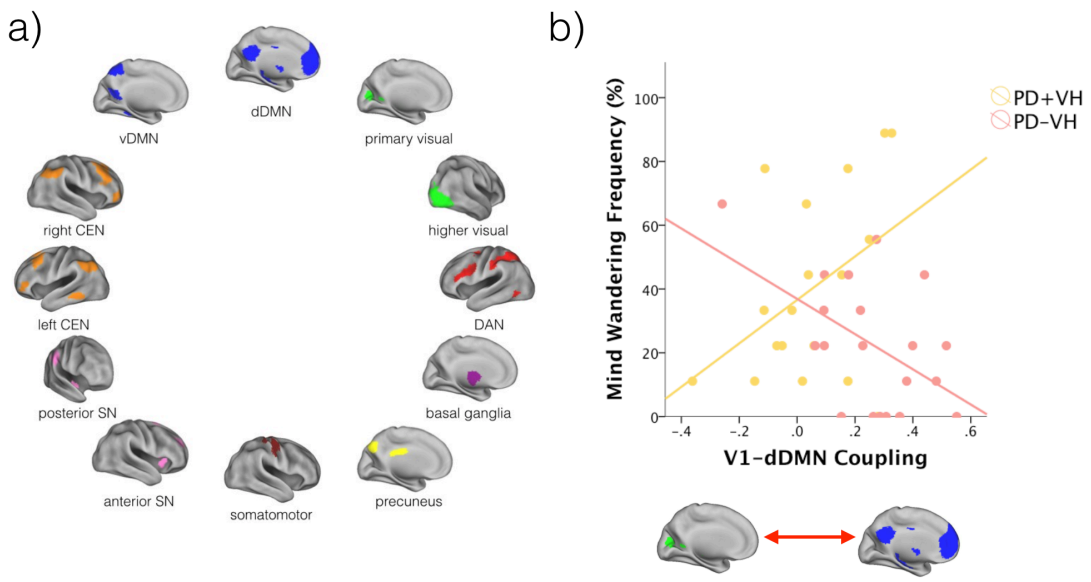

Figure 4. ***Association between mind-wandering frequency and inter-network coupling.*** a) Stanford atlas networks included in the analysis examining the association between inter-network functional connectivity and mind-wandering frequency; b) Individuals with visual hallucinations (PD+VH) had a significantly stronger association between mind-wandering frequency and V1-dDMN coupling, compared to those without hallucinations (PD-VH). dDMN = dorsal default mode network; vDMN = ventral default mode network; CEN = central executive network; SN = salience network; DAN = dorsal attention network

Follow-up seed-to-voxel functional connectivity with a V1 seed

When the primary visual network was used as a seed, the between-group difference in the association between V1 coupling and mind-wandering frequency included brain regions both within and beyond the dorsal default mode network. Relative to PD-VH, PD+VH displayed a significantly stronger association between mind-wandering frequency and connectivity of the V1 seed to dDMN regions (posterior cingulate cortex, medial prefrontal cortex, temporoparietal junction, and angular gyrus), the inferior frontal gyrus, and high-level visual regions (fusiform gyrus/inferior temporal gyrus). See Figure 5 and Table 2.

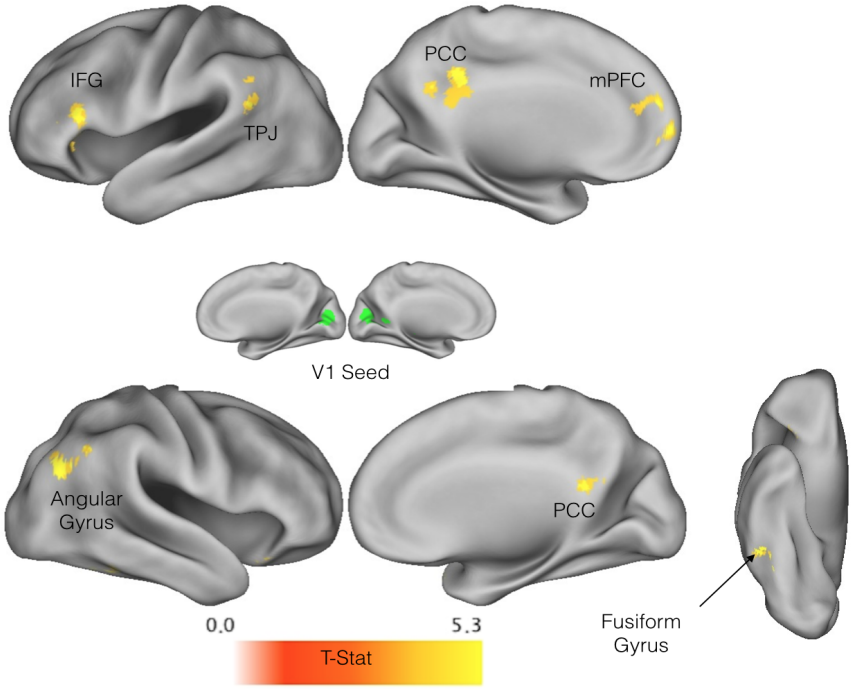

Figure 5. ***Seed-to-voxel connectivity between V1 seed and whole brain.*** Individuals with hallucinations had a significantly stronger association between mind-wandering frequency and connectivity between VI and areas of the dorsal default mode network (PCC, mPFC and TPJ/angular gyrus), the inferior frontal gyrus, and high-level visual regions (fusiform gyrus/inferior temporal gyrus), relative to non-hallucinating individuals. PCC = posterior cingulate cortex; mPFC = medial prefrontal cortex; TPJ = temporoparietal junction; IFG = inferior frontal gyrus.

Table 2. Peak coordinates from seed-to-voxel analysis

Brain Region	x y z	Voxels
R Inferior Orbital Cortex	40 24 -24	122
L Inferior Frontal Gyrus	-50 26 12	209
L Medial Prefrontal Cortex	-16 54 00	136
	-06 54 18	163
R Fusiform Gyrus	50 -46 -24	91
L Posterior Cingulate Cortex	-10 -42 36	313
L Inferior Parietal Lobule	-44 -46 26	290
R Angular Gyrus	48 -66 32	122
L Midbrain	-08 -24 -04	98

R = right; L = left; x, y, z = co-ordinates in MNI standard space.

Mind-wandering frequency covaries with grey matter volume in the posterior parietal cortex in non-hallucinating individuals

A significant interaction was identified between mind-wandering frequency in the PD-VH group and grey matter volume in the left posterior parietal lobe. The cluster spanned both inferior and superior regions of the posterior parietal lobe (see Figure 6a). To determine directionality of the significant interaction, a correlation analysis was conducted in the PD-VH group, between mind-wandering frequency and mean grey matter intensity values extracted from the significant cluster. A significant positive relationship emerged ($r = 0.75$, $p < 0.001$; see Supplementary Figure S3), consistent with an association between grey matter loss in the posterior parietal cortex in PD-VH and reduced mind-wandering. There were no regions where grey matter volume covaried significantly with mind-wandering performance in the PD+VH group. Main effects are not reported/interpreted due to the significant interaction.

Of the 12 networks from the Stanford atlas applied to the resting state data, the identified cluster showed overlap with three: the precuneus network, left executive control network, and the ventral default network. The cluster showed equal overlap with the precuneus and LECN networks (GOF = 0.32) and less overlap with the vDMN (GOF = 0.01; see Figure 6b). In supplementary Figure S4 we illustrate the proximity of our identified grey matter cluster to a meta-analytic cluster revealed in a meta-analysis of functional neuroimaging studies of mind-wandering in healthy people (Fox *et al.*, 2015).

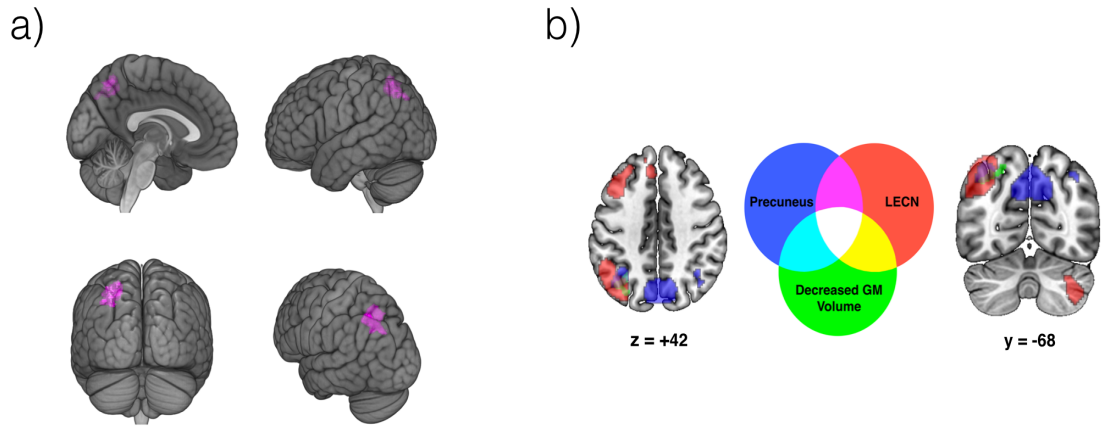

Figure 6. ***Voxel-based morphometry results and overlap with intrinsic functional networks.*** a) A significant cluster in the left posterior parietal cortex showed a positive correlation with mind-wandering frequency in the non-hallucinating group. Cluster size = 495 voxels; MNI coordinates of maxima: x = -28, y -76, z = 38. Result corrected for cluster mass at $p < 0.05$ and a cluster forming threshold of T = 3; b) The identified cluster showed greatest overlap with two intrinsic functional networks derived from the Stanford atlas. Significant grey matter cluster shown in green; left executive control network (LECN) shown in red, and precuneus network shown in blue.

Discussion

Our results provide empirical evidence of a link between mind-wandering and visual hallucinations, revealing that PD patients with hallucinations exhibit increased mind-wandering relative to non-hallucinating patients. It follows that elevated levels of mind-wandering may be a cognitive correlate of the excessive top-down influences on perception that have been hypothesised in PD visual hallucinations. Our resting state analysis revealed a route by which mind-wandering may impact upon early visual processing, as mind-wandering frequency was associated with stronger coupling between the primary visual and dorsal default mode networks in PD hallucinators. Together, these findings uncover trait characteristics: increased mind-wandering

frequency related to default mode-visual network coupling, which may predispose the Parkinsonian brain to hallucinate.

Our behavioural results showed that mind-wandering frequency was significantly higher in the hallucinating group (PD+VH) compared to the non-hallucinating group, and was at a similar level to controls. In contrast, the frequency of mind-wandering was reduced in non-hallucinating PD patients (PD-VH) relative to controls, replicating an independent PD cohort tested on the same task (Geffen *et al.*, 2017). Global cognitive function does not appear to account for the higher levels of mind-wandering in PD+VH, as their cognitive abilities were either similar to PD-VH, or mildly reduced. Instead, combined with the resting state results, our findings suggest that patterns of increased coupling between the primary visual and dorsal default mode network may mediate higher levels of mind-wandering in PD+VH. In contrast, grey matter changes in the posterior parietal cortex were associated with reduced mind-wandering, specifically in the non-hallucinating phenotype. These findings suggest that while primarily functional changes may support increased mind-wandering in PD+VH, underlying structural changes contribute to the reduced mind-wandering in PD-VH.

In the PD+VH group, mind-wandering frequency increased as a function of V1-dDMN coupling (i.e., they were positively correlated). In healthy people, primary sensory regions are typically not involved in mind-wandering (Fox *et al.*, 2015), consistent with the notion that directing attention away from external sensory input is essential to facilitate mind-wandering (Schooler *et al.*, 2011, Smallwood and Schooler, 2015). This implies a functional separation between the DMN and primary sensory areas, such as V1, in relation to mind-wandering. Such a pattern would be consistent with the relationship identified in the PD-VH group, where increased rates of mind-wandering were linked to a relative *decoupling* of the V1 and dDMN networks. The relationship observed in PD+VH is the opposite of what might be predicted based on healthy control data: increased rates of mind-wandering reflected greater coupling between the dDMN and a primary sensory region, V1. This suggests that whilst mind-wandering in PD+VH was maintained at the level of controls, it is likely to be supported by different cognitive or neural resources, and possibly accompanied by a different (i.e., more visual) phenomenology. An important future

direction will be to establish the phenomenological characteristics of increased mind-wandering in PD+VH, to determine whether the thought content is primarily visual, and the extent to which it is dynamic and unconstrained.

Post-hoc seed-to-voxel analysis confirmed a significant group difference in the association between mind-wandering frequency and connectivity between V1 and the dDMN (PCC, mPFC, right TPJ and left angular gyrus). This analysis enabled a more specific localisation of regions that might mediate the relationship between mind-wandering and V1 connectivity. Our findings implicated specific regions within the DMN, including the mPFC, previously been identified as a source of top-down influence over visual perception (Bar *et al.*, 2006, Summerfield *et al.*, 2006, Kveraga *et al.*, 2007). Regions outside the DMN were also identified, including the fusiform gyrus/inferior temporal gyrus, a higher-level region in the ventral visual processing stream; and, the inferior frontal gyrus, which has been identified (via effective connectivity) as a source of directed top-down influence over V1 during both mental imagery and perception (Dijkstra *et al.*, 2017).

In contrast to the resting-state connectivity changes implicated in mind-wandering and PD+VH, voxel-based morphometry revealed that grey matter loss in the left posterior parietal cortex was associated with reduced mind-wandering frequency in PD-VH. As confirmed by our goodness-of-fit analysis, this region is adjacent to large-scale functional networks important for mind-wandering in healthy people (i.e., default mode and cognitive control networks) (Fox *et al.*, 2015). The left posterior parietal cortex is also consistently found to be activated during mental imagery (Winlove *et al.*, 2018). This raises the possibility that reduced mind-wandering and reduced mental imagery may be common features of the non-hallucinating phenotype in PD, which are mediated, at least in part, by grey matter loss in the posterior parietal cortex. We suggest that in PD more broadly, disease-related patterns of posterior parietal cortical grey matter loss could contribute to reductions in mind-wandering. However, in certain cases where mind-wandering or mental imagery is elevated in association with increased V1-default mode network coupling, this will be linked to an hallucinating phenotype.

Based on patterns of functional connectivity across the entire cerebral cortex, the DMN is located on the opposite end of a principal connectivity gradient from brain regions supporting primary perceptual processing (e.g., the primary visual network) (Margulies *et al.*, 2016, Huntenburg *et al.*, 2017, Murphy *et al.*, 2018). Our results suggest that, in PD+VH, an elevated level of mind-wandering is associated with a loss of this inherent functional separation between the DMN and V1. This is consistent with a previous task-based study, which found increased visual network coupling to the DMN during misperceptions in PD+VH (Shine *et al.*, 2015b). A combination of increased internally generated thought and imagery, and increased influence from the DMN over early visual regions, may therefore comprise a neurocognitive endophenotype that is prone to hallucinate. Intriguingly, increased psychopathological features in the general population have been associated with elevated visual network-DMN coupling (Elliott *et al.*, 2018), suggesting that the loss of functional segregation between these networks may play a role across neuropsychiatric disorders.

Our findings are consistent with models of visual hallucinations in PD that specify an overabundance of influence from top-down regions during visual processing. In PD, it is still unclear what neurotransmitter systems might mediate such an imbalance. Dopamine and acetylcholine are thought to play complementary roles during perceptual inference, as dopamine may encode low-level sensory prediction errors, while cholinergic function determines the balance between top-down vs. bottom up influences, by modulating information flow across ascending and descending intra-cortical circuitry (Iglesias *et al.*, 2017). Under the influence of the psychedelic compound lysergic acid diethylamide (LSD), increased V1 coupling to regions within the DMN has been shown to correlate with complex visual hallucinations (Carhart-Harris *et al.*, 2016). This finding is particularly intriguing considering LSD is a potent 5-HT_{2A} agonist and a recently approved treatment for psychosis in PD, pimavanserin, is a 5-HT_{2A} inverse agonist (Cummings *et al.*, 2014). Given that these neuromodulatory systems are all variably affected in individuals with PD, identifying their respective roles in modulating top-down vs. bottom-up imbalances in PD hallucinations may open further therapeutic avenues.

In summary, our study has identified a behavioural consequence of the DMN abnormalities previously documented in PD hallucinations, namely increased mind-

wandering frequency. To our knowledge, these findings provide the first evidence of a relationship between mind-wandering and visual hallucinations in a clinical population. Higher levels of mind-wandering indicate an increased propensity for mental imagery, formation of contextual associations and spontaneous thought, all top-down processes that could furnish the content of visual hallucinations. Our results suggest a putative neural substrate that supports excessive influence from these top-down processes over perception, by way of increased coupling between the DMN and early visual regions. Elevated mind-wandering in association with loss of segregation between primary sensory and transmodal neural networks, offers a specific neurocognitive marker for top-down influences that may contribute to hallucinations across disorders.

Acknowledgments:
We thank Kieran Fox for providing us with a mask to visualise the mind-wandering meta-analytic results, and Kelly Diederen for providing valuable comments on the manuscript. AJM is supported by an Australian Postgraduate Award through the University of Sydney. JMH is supported by a Western Sydney University Postgraduate Award. JAH is supported by the University of Arizona and a grant from the John Templeton Foundation, "Prospective Psychology Stage 2: A Research Competition" to Martin Seligman. The opinions expressed in this publication are those of the author(s) and do not necessarily reflect the views of the John Templeton Foundation. MI is supported by an Australian Research Council Future Fellowship (FT160100096). SJGL is supported by an NHMRC-ARC Dementia Fellowship (#1110414). JMS is supported by a National Health and Medical Research Council CJ Martin Fellowship (1072403). CO is supported by a National Health and Medical Research Council Neil Hamilton Fairley Fellowship (1091310) and by the Wellcome Trust (200181/Z/15/Z). The study was supported by a Seed Grant from Parkinson's NSW and funding to Forefront, a collaborative research group dedicated to the study of non-Alzheimer disease degenerative dementias, from the National Health and Medical Research Council of Australia program grant (#1037746 and #1095127).

Conflict of interest disclosure: The authors report no conflicts of interest.

Figure Legends:

Figure 1

Title – Task structure and schematic of scoring system

Legend – a) An example of two trials in the thought sampling task; b) Responses were scored from 1-4, with 1 consisting of a stimulus bound response, such as reporting thoughts about the displayed shape, and 4 corresponding to thoughts completely unrelated to the task or immediate environment.

Figure 2

Title – Mind-wandering frequency

Legend – PD with hallucinations (PD+VH) and controls both showed higher frequencies of mind-wandering (i.e., had significantly more Level 4 responses on the thought sampling task) compared to non-hallucinators (PD-VH). Error bars show standard error of the mean; n.s. = not significant; * = $p < .05$.

Figure 3

Title – Frequency of responses at each of the four scoring levels

Legend – Group differences were only found for Level 4 responses (i.e., mind-wandering frequency). Frequencies of responses across the three groups were not significantly different for Levels 1, 2 and 3. Error bars show standard error of the mean; PD-VH = non-hallucinators; PD+VH = hallucinators; n.s. = not significant; * = $p < 0.05$.

Figure 4

Title – Association between mind-wandering frequency and inter-network coupling

Legend – a) Stanford atlas networks included in the analysis examining the association between inter-network functional connectivity and mind-wandering frequency; b) Individuals with visual hallucinations (PD+VH) had a significantly stronger association between mind-wandering frequency and V1-dDMN coupling, compared to those without hallucinations (PD-VH). dDMN = dorsal default mode network; vDMN = ventral default mode network; CEN = central executive network; SN = salience network; DAN = dorsal attention network

Figure 5

Title – Seed-to-voxel connectivity between V1 seed and whole brain

Legend – Individuals with hallucinations had a significantly stronger association between mind-wandering frequency and connectivity between VI and areas of the dorsal default mode network (PCC, mPFC and TPJ/angular gyrus), the inferior frontal gyrus, and high-level visual regions (fusiform gyrus), relative to non-hallucinating individuals. PCC = posterior cingulate cortex; mPFC = medial prefrontal cortex; TPJ = temporoparietal junction; IFG = inferior frontal gyrus.

Figure 6

Title – Voxel-based morphometry results and overlap with intrinsic functional networks.

Legend – a) A significant cluster in the left posterior parietal cortex showed a positive correlation with mind-wandering frequency in the non-hallucinating group. Cluster size = 495 voxels; MNI coordinates of maxima: x = -28, y -76, z = 38. Result corrected for cluster mass at $p < 0.05$ and a cluster forming threshold of T = 3; b) The identified cluster showed greatest overlap with two intrinsic functional networks derived from the Stanford atlas. Significant grey matter cluster shown in green; left executive control network (LECN) shown in red, and precuneus network shown in blue.

References

Adams RA, Stephan KE, Brown HR, Frith CD, Friston KJ. The computational anatomy of psychosis. Frontiers in psychiatry. 2013;4:47.

Aminoff EM, Kveraga K, Bar M. The role of the parahippocampal cortex in cognition. Trends in Cognitive Sciences. 2013;17(8):379-90.

Andrews-Hanna JR, Reidler JS, Sepulcre J, Poulin R, Buckner RL. Functional-anatomic fractionation of the brain's default network. Neuron. 2010;65(4):550-62.

Bar M, Kassam KS, Ghuman AS, Boshyan J, Schmid AM, Dale AM, et al. Top-down facilitation of visual recognition. Proceedings of the National Academy of Sciences of the United States of America. 2006;103(2):449-54.

Bates D, Mächler M, Bolker B, Walker S. Fitting linear mixed-effects models using lme4. arXiv preprint arXiv:14065823. 2014.

Beck AT, Steer RA, Brown GK. Beck depression inventory-II. San Antonio. 1996;78(2):490-8.

Bell AH, Summerfield C, Morin EL, Malecek NJ, Ungerleider LG. Encoding of stimulus probability in macaque inferior temporal cortex. Current Biology. 2016;26(17):2280-90.

Buckner RL, Andrews-Hanna JR, Schacter DL. The brain's default network. Annals of the New York Academy of Sciences. 2008;1124(1):1-38.

Cardinal RN, Aitken MR. ANOVA for the behavioral sciences researcher: Psychology Press; 2013.

Carhart-Harris RL, Muthukumaraswamy S, Roseman L, Kaelen M, Droog W, Murphy K, et al. Neural correlates of the LSD experience revealed by multimodal neuroimaging. Proceedings of the National Academy of Sciences. 2016;113(17):4853-8.

Christoff K, Irving ZC, Fox KC, Spreng RN, Andrews-Hanna JR. Mind-wandering as spontaneous thought: a dynamic framework. Nature Reviews Neuroscience. 2016;17(11):718-31.

Collerton D, Perry E, McKeith I. Why people see things that are not there: a novel perception and attention deficit model for recurrent complex visual hallucinations. Behavioral and Brain Sciences. 2005;28(06):737-57.

Collerton D, Taylor J-P, Tsuda I, Fujii H, Nara S, Aihara K, et al. How can we see things that are not there?: current insights into complex visual hallucinations. Journal of Consciousness Studies. 2016;23(7-8):195-227.

Cummings J, Isaacson S, Mills R, Williams H, Chi-Burris K, Corbett A, et al. Pimavanserin for patients with Parkinson's disease psychosis: a randomised, placebo-controlled phase 3 trial. The Lancet. 2014;383(9916):533-40.

Dalrymple-Alford J, MacAskill M, Nakas C, Livingston L, Graham C, Crucian G, et al. The MoCA well-suited screen for cognitive impairment in Parkinson disease. Neurology. 2010;75(19):1717-25.

Diederich NJ, Goetz CG, Stebbins GT. Repeated visual hallucinations in Parkinson's disease as disturbed external/internal perceptions: focused review and a new integrative model. Movement Disorders. 2005;20(2):130-40.

Dijkstra N, Zeidman P, Ondobaka S, Gerven M, Friston K. Distinct top-down and bottom-up brain connectivity during visual perception and imagery. Scientific reports. 2017;7(1):5677.

Elliott ML, Romer A, Knodt AR, Hariri AR. A Connectome Wide Functional Signature of Transdiagnostic Risk for Mental Illness. Biological Psychiatry. 2018.

ffytche D, Creese B, Politis M, Chaudhuri KR, Weintraub D, Ballard C, et al. The psychosis spectrum in Parkinson disease. Nature Reviews Neurology. 2017;13(2):81.

Fletcher PC, Frith CD. Perceiving is believing: a Bayesian approach to explaining the positive symptoms of schizophrenia. Nature Reviews Neuroscience. 2009;10(1):48-58.

Fox KC, Spreng RN, Ellamil M, Andrews-Hanna JR, Christoff K. The wandering brain: Meta-analysis of functional neuroimaging studies of mind-wandering and related spontaneous thought processes. NeuroImage. 2015;111:611-21.

Franciotti R, Delli Pizzi S, Perfetti B, Tartaro A, Bonanni L, Thomas A, et al. Default mode network links to visual hallucinations: A comparison between Parkinson's disease and multiple system atrophy. Movement Disorders. 2015;30(9):1237-47.

Friston KJ. Hallucinations and perceptual inference. Behavioral and Brain Sciences. 2005;28(06):764-6.

Geffen T, Thaler A, Gilam G, Simon EB, Sarid N, Gurevich T, et al. Reduced mind wandering in patients with Parkinson's disease. Parkinsonism & related disorders. 2017;44:38-43.

Gilbert CD, Li W. Top-down influences on visual processing. Nature Reviews Neuroscience. 2013;14(5):350.

Goetz CG, Tilley BC, Shaftman SR, Stebbins GT, Fahn S, Martinez‐Martin P, et al. Movement Disorder Society‐sponsored revision of the Unified Parkinson's Disease Rating Scale (MDS‐UPDRS): Scale presentation and clinimetric testing results. Movement disorders. 2008;23(15):2129-70.

Guo CC, Tan R, Hodges JR, Hu X, Sami S, Hornberger M. Network-selective vulnerability of the human cerebellum to Alzheimer’s disease and frontotemporal dementia. Brain. 2016;139(5):1527-38.

Hindy NC, Ng FY, Turk-Browne NB. Linking pattern completion in the hippocampus to predictive coding in visual cortex. Nature neuroscience. 2016;19(5):665.

Huntenburg JM, Bazin P-L, Margulies DS. Large-Scale Gradients in Human Cortical Organization. Trends in cognitive sciences. 2017.

Iglesias S, Tomiello S, Schneebeli M, Stephan KE. Models of neuromodulation for computational psychiatry. Wiley Interdisciplinary Reviews: Cognitive Science. 2017;8(3).

Irving ZC. Mind-wandering is unguided attention: accounting for the "purposeful" wanderer. Philosophical Studies. 2016;173(2):547-71.

Kok P. Perceptual Inference: A Matter of Predictions and Errors. Current Biology. 2016;26(17):R809-R11.

Kucyi A. Just a thought: How mind-wandering is represented in dynamic brain connectivity. NeuroImage. 2017.

Kveraga K, Boshyan J, Bar M. Magnocellular projections as the trigger of top-down facilitation in recognition. Journal of Neuroscience. 2007;27(48):13232-40.

Kveraga K, Ghuman AS, Kassam KS, Aminoff EA, Hämäläinen MS, Chaumon M, et al. Early onset of neural synchronization in the contextual associations network. Proceedings of the National Academy of Sciences. 2011;108(8):3389-94.

Margulies DS, Ghosh SS, Goulas A, Falkiewicz M, Huntenburg JM, Langs G, et al. Situating the default-mode network along a principal gradient of macroscale cortical organization. Proceedings of the National Academy of Sciences. 2016;113(44):12574-9.

Murphy C, Jefferies E, Rueschemeyer S-A, Sormaz M, Wang H-t, Margulies DS, et al. Distant from input: Evidence of regions within the default mode network supporting perceptually-decoupled and conceptually-guided cognition. NeuroImage. 2018.

O'Callaghan C, Shine J, Hodges J, Andrews-Hanna J, Irish M. Hippocampal atrophy and intrinsic brain network alterations relate to impaired capacity for mind wandering in neurodegeneration. bioRxiv. 2017:194092.

O'Callaghan C, Hall JM, Tomassini A, Muller AJ, Walpola IC, Moustafa AA, et al. Visual hallucinations are characterized by impaired sensory evidence accumulation: Insights from hierarchical drift diffusion modeling in Parkinson's disease. Biological Psychiatry: Cognitive Neuroscience and Neuroimaging. 2017a;2(8):680-8.

O'Callaghan C, Kveraga K, Shine JM, Adams Jr RB, Bar M. Predictions penetrate perception: Converging insights from brain, behaviour and disorder. Consciousness and cognition. 2017b;47:63-74.

O'Callaghan C, Shine JM, Lewis SJ, Andrews-Hanna JR, Irish M. Shaped by our thoughts–A new task to assess spontaneous cognition and its associated neural correlates in the default network. Brain and cognition. 2015;93:1-10.

Phillips N. yarrr: A companion to the e-book YaRrr!: The Pirate's Guide to R. R package version 01. 2016.

Power JD, Barnes KA, Snyder AZ, Schlaggar BL, Petersen SE. Spurious but systematic correlations in functional connectivity MRI networks arise from subject motion. Neuroimage. 2012;59(3):2142-54.

Powers AR, Kelley M, Corlett PR. Hallucinations as top-down effects on perception. Biological Psychiatry: Cognitive Neuroscience and Neuroimaging. 2016;1(5):393-400.

Schacter DL, Addis DR, Hassabis D, Martin VC, Spreng RN, Szpunar KK. The future of memory: remembering, imagining, and the brain. Neuron. 2012;76(4):677-94.

Schooler JW, Smallwood J, Christoff K, Handy TC, Reichle ED, Sayette MA. Meta-awareness, perceptual decoupling and the wandering mind. Trends in Cognitive Sciences. 2011;15(7):319-26.

Seli P, Kane MJ, Smallwood J, Schacter DL, Maillet D, Schooler JW, et al. Mind-wandering as a natural kind: A family-resemblances view. Trends in cognitive sciences. 2018;22(6):479-90.

Shin D-J, Lee TY, Jung WH, Kim SN, Jang JH, Kwon JS. Away from home: the brain of the wandering mind as a model for schizophrenia. Schizophrenia research. 2015;165(1):83-9.

Shine JM, Keogh R, O'Callaghan C, Muller AJ, Lewis SJ, Pearson J. Imagine that: elevated sensory strength of mental imagery in individuals with Parkinson's disease and visual hallucinations. Proc R Soc B. 2015a;282(1798):20142047.

Shine JM, Muller AJ, O’Callaghan C, Hornberger M, Halliday GM, Lewis SJ. Abnormal connectivity between the default mode and the visual system underlies the manifestation of visual hallucinations in Parkinson’s disease: a task-based fMRI study. npj Parkinson's Disease. 2015b;1:15003.

Shine JM, O'Callaghan C, Halliday GM, Lewis SJG. Tricks of the mind: Visual hallucinations as disorders of attention. Progress in Neurobiology. 2014;116:58-65.

Shirer W, Ryali S, Rykhlevskaia E, Menon V, Greicius MD. Decoding subject-driven cognitive states with whole-brain connectivity patterns. Cerebral cortex. 2012;22(1):158-65.

Smallwood J, Schooler JW. The science of mind wandering: empirically navigating the stream of consciousness. Annual review of psychology. 2015;66:487-518.

Smith SM. Fast robust automated brain extraction. Human brain mapping. 2002;17(3):143-55.

Spreng RN, Mar RA, Kim AS. The common neural basis of autobiographical memory, prospection, navigation, theory of mind, and the default mode: a quantitative meta-analysis. Journal of cognitive neuroscience. 2009;21(3):489-510.

Summerfield C, Egner T, Greene M, Koechlin E, Mangels J, Hirsch J. Predictive codes for forthcoming perception in the frontal cortex. Science. 2006;314(5803):1311-4.

Weil RS, Schrag AE, Warren JD, Crutch SJ, Lees AJ, Morris HR. Visual dysfunction in Parkinson's disease. Brain. 2016;139(11):2827-43.

Whitfield-Gabrieli S, Nieto-Castanon A. Conn: a functional connectivity toolbox for correlated and anticorrelated brain networks. Brain connectivity. 2012;2(3):125-41.

Winlove C, Milton F, Ranson J, Fulford J, MacKisack M, Macpherson F, et al. The neural correlates of visual imagery: a co-ordinate-based meta-analysis. Cortex. 2018.

Yao N, Shek-Kwan Chang R, Cheung C, Pang S, Lau KK, Suckling J, et al. The default mode network is disrupted in Parkinson's disease with visual hallucinations. Human brain mapping. 2014;35(11):5658-66.

Zabelina DL, Andrews-Hanna JR. Dynamic network interactions supporting internally-oriented cognition. Current Opinion in Neurobiology. 2016;40:86-93.

Zhang Y, Brady M, Smith S. Segmentation of brain MR images through a hidden Markov random field model and the expectation-maximization algorithm. IEEE transactions on medical imaging. 2001;20(1):45-57.